

SCIENTIFIC REPORTS



OPEN

Hypometabolism during Daily Torpor in Mice is Dominated by Reduction in the Sensitivity of the Thermoregulatory System

Genshiro A. Sunagawa & Masayo Takahashi

Received: 22 August 2016

Accepted: 21 October 2016

Published: 15 November 2016

Some mammals enter a hypometabolic state either daily torpor (minutes to hours in length) or hibernation (days to weeks), when reducing metabolism would benefit survival. Hibernators demonstrate deep torpor by reducing both the sensitivity (H) and the theoretical set-point temperature (T_R) of the thermogenesis system, resulting in extreme hypothermia close to ambient temperature. However, these properties during daily torpor remain poorly understood due to the very short steady state of the hypometabolism and the large variation among species and individuals. To overcome these difficulties in observing and evaluating daily torpor, we developed a novel torpor-detection algorithm based on Bayesian estimation of the basal metabolism of individual mice. Applying this robust method, we evaluated fasting induced torpor in various ambient temperatures (T_{AS}) and found that H decreased 91.5% during daily torpor while T_R only decreased 3.79 °C in mice. These results indicate that thermogenesis during daily torpor shares a common property of sensitivity reduction with hibernation while it is distinct from hibernation by not lowering T_R . Moreover, our findings support that mice are suitable model animals to investigate the regulation of the heat production during active hypometabolism, thus suggesting further study of mice may provide clues to regulating hypometabolism in mammals.

Mammals and birds evolutionarily gained homeothermicity (a constant T_B) to keep the animal's internal environment stable despite changes in the outer environment. The ability to maintain a stable environment inside the body allowed species the freedom to spread widely over various regions with differing environments. While providing the freedom to prosper, homeothermicity entails a huge metabolic cost. Small animals, which have a high temperature conductance compared to larger animals, spend a larger portion of their metabolism on thermogenesis¹ and must produce more heat relative to their size to keep a constant T_B . This is thought to be the reason why active hypometabolism is seen mainly in relatively small animals². Based on the duration of the torpid status, active hypometabolism is called daily torpor or hibernation (deep torpor), which are daily base or seasonal base, respectively. Any kind of active hypometabolism reduces the demand for oxygen by giving up various vital functions and the animal becomes immobile and unresponsive. Some small animals evolved to take these risks rather than traveling aggressively to find food. Although active hypometabolism might appear to represent an evolutionary regression, it is a functional adaptation for overcoming situations that have become critical due to the high oxygen demands of homeothermicity. Four conditions are required for a euthermic animal to undergo hypometabolism, and the mechanisms of none of them are clearly known. First, the animal must turn off or at least suppress the thermoregulatory system during active hypometabolism. During hypometabolism, the animal reaches a hypothermic state that would trigger thermogenesis under normal conditions. If the normal thermoregulatory mechanism is not modified, additional energy will be spent rather than saved—which is clearly undesirable during hypometabolism. Second, the animal must be able to endure low respiration levels or low oxygen supply. Euthermic animals are designed to maintain life with a certain oxygen supply; however, in some small animals, the oxygen consumption during hibernation is reduced to 2–3% of that in an aroused state³. The animals have to maintain their vital metabolism under scarce oxygen conditions. Third, the animal must be resistant to

Laboratory for Retinal Regeneration, RIKEN Center for Developmental Biology, 2-2-3 Minatojima-minami-machi, Chuo-ku, Kobe, Hyogo 650-0047, Japan. Correspondence and requests for materials should be addressed to G.A.S. (email: genshiro.sunagawa@riken.jp)

hypothermia. Mammals maintain a constant T_B . However, hibernators typically have a minimum T_B of 2–10 °C⁴. Non-hibernator mammalian tissues are usually damaged under such hypothermic state by disturbances in cellular ion homeostasis triggered by alterations in membrane fluidity⁵. Moreover, rewarming from hypothermia is also known to induce cellular stress response⁶. These hypothermia related responses must be prevented during and after hypometabolism. Fourth, the animal must be able to return to a normal metabolic state by producing heat from a hypometabolic state, and to tolerate this rise in heat. Animals in daily torpor or hibernation return to a euthermic state over a period of several hours⁷. This is striking in two points: 1) warming begins with the animal in a hypometabolic state in which it cannot produce heat as usual, and 2) live cells cannot usually survive such a rapid thermal change.

Among the four conditions of hypometabolism, the modification of the thermoregulatory system during active hypometabolism have been the centre of interest for a long time^{8–13}. One issue that has been discussed in this field is the determination of the main effector of hypometabolism. What components of the thermoregulatory system are involved in hypometabolism? There are three possibilities; the heat conductance of the body (G), the reference of the body temperature (T_R) and the open-loop gain of the thermoregulatory feedback system (H). G is the major factor responsible for how easy the heat is lost. It is largely determined by skin blood flow and body surface area. T_R is a reference temperature or the theoretical set-point of body temperature, which the system is targeting to. Although, the word ‘set-point’ is less frequently used due to the discovery of multiple mechanisms governing the body temperature in a multiple target temperatures^{14,15}, in this article we use the term ‘set-point’ to express the temperature that the thermoregulation system is driving toward to by combining various mechanisms to keep the core body temperature stable. H is another theoretical parameter describing the open-loop gain of the thermoregulatory negative feedback system. The gain of the negative feedback determines the degree of effectiveness with which a control system maintains constant conditions¹⁶. In this system, when the H is larger, T_B tends to become closer to T_R . Considering these components, when the animal is not moving, in other words, when the animals’ external work is negligible, a block diagram for thermoregulation can be written as Fig. 1a. Several groups have investigated the dynamics of these parameters in hibernators and reported that reduction is seen in both T_R and H ^{8,9,17}. The basic approach in hibernators is to observe various metabolic states during deep torpor while controlling T_A and to estimate the parameters. Usually, the stable torpid period in hibernators last for days which allow testing multiple conditions during a single torpor bout. On the other hand, these parameters in daily torpor are not known. This is because in daily torpor, the period of stable hypometabolism, which is the period when the VO_2 and T_B are stable, last only for minutes to hours. This is preventing to perform multiple observations of metabolism at various T_A s, which is not difficult in hibernators because they have days of stable torpid periods. To reveal the degree to which the three factors contribute to hypometabolism in daily torpor, we chose to investigate the house mouse, *Mus musculus*, which is not only one of the most popular laboratory animals, but it is also capable of entering daily torpor^{18,19}. To overcome the metabolism recording difficulties in torpid animals, in this study, we first built a system to simultaneously record the oxygen consumption and body temperature of a freely-moving mouse. To evaluate metabolism quantitatively and objectively during daily torpor, we developed a fully automated hypometabolism-detection algorithm based on Bayesian inference. Observing the normal and torpid mouse in various T_A s, we estimated the parameters of the thermoregulatory system to elucidate the factors determining hypothermia during daily torpor.

Results

System for recording the metabolism of free-moving mice under controlled ambient temperature. Many studies have reported that lowering the T_A and restricting food can induce daily torpor in mice^{10,20–23}. However, most of these studies used a wired temperature-recording system and a small metabolism chamber to evaluate the animal, which may alter the animal’s phenotype, especially for small animals. Furthermore, the sex, age, and strain of the model animal differed among studies, making them difficult to compare. Therefore, to understand the mechanism of daily torpor in mice, we first sought to develop an efficient, minimally invasive system to evaluate their metabolism. We prepared a chamber in which the T_A could be controlled (Fig. 1b); the standard deviation of the difference between T_A and the target temperature was less than 1 °C (Supplementary Fig. 1a). We set up a long-term metabolism analyser and a wireless T_B -monitoring system (Fig. 1b) in the thermo-controlled chamber, and successfully recorded the animals’ VO_2 and T_B continuously for more than three days without any physical contact with the animal (Fig. 1c). We used networked cameras to closely monitor each animal’s appearance and health status. To determine a stable and efficient condition for inducing daily torpor, we used the inbred laboratory strain C57BL/6J, which can enter torpor under certain conditions¹⁸. To reduce phenotype variance as much as possible, we only used male mice between 7 and 9 weeks of age. When water remained freely available but food was removed for 24 hours under a constant T_A (Fig. 1d; the filled and open triangles at the top denote food removal and return, respectively), a typical torpid episode began on the latter half of the same day (Fig. 1d, Supplementary Fig. 1b,c and Supplementary Movies 1, 2 and 3). Because past studies have used various definitions of daily torpor, we sought to define daily torpor based on statistical prediction of the individual metabolism of the animal.

Modelling and predicting metabolism from a single day recording. Past reports have defined daily torpor by a threshold T_B or VO_2 ^{10,22} or a minimal T_B or VO_2 ²³, but these thresholds vary from study to study. Furthermore, the dynamics of T_B and VO_2 vary greatly between individuals (Fig. 2a,b). To overcome the metabolic variance observed between different individuals and environments, we propose a statistical approach to detect the individual baseline metabolism and to define daily torpor as an outlier of the baseline metabolism.

Hence, we modelled the time-series dynamics of both T_B and VO_2 with a second-order trend model using Bayesian estimation (Fig. 2c,d and Supplementary Fig. 2a,b; see Methods). We used data acquired from non-torpid mice ($n = 4$, $T_A = 16$ °C, mice 5 to 8) for three days, and estimated σ_2 , the standard deviation of the

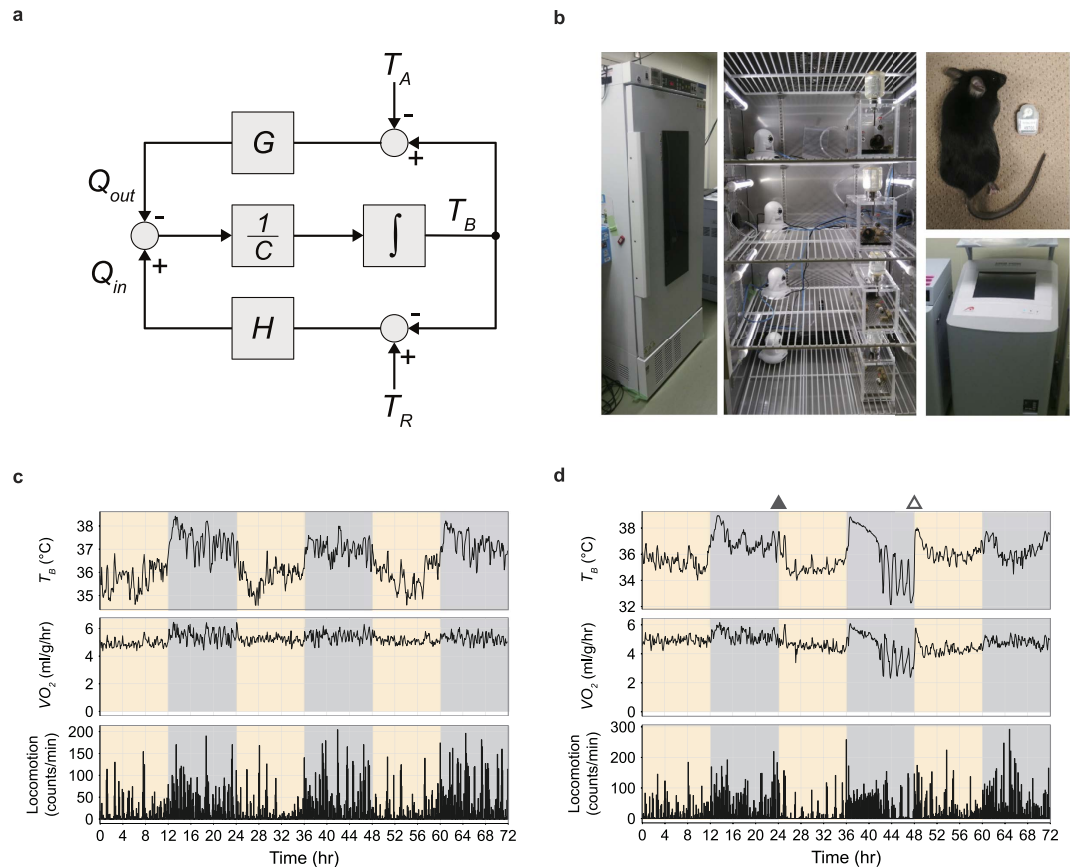


Figure 1. System for recording the metabolism of free-moving mice under controlled ambient temperature. (a) A block diagram of the thermoregulatory system in mammals when the animal is not moving, therefore assumed to exert no external work. The upper loop and the lower loop represent the heat loss and heat production loop, respectively. The time derivative of body temperature (T_B) is derived from the difference of heat production (Q_{in}) and heat loss (Q_{out}) divided by the thermal capacity (C). Q_{out} is derived from the difference of ambient temperature (T_A) and T_B multiplied by heat conductance (G). Q_{in} is derived from the difference of theoretically defined set-point temperature (T_R) and T_B multiplied by H , which is the open-loop gain of the thermoregulatory feedback system. (b) A system for evaluating the metabolism of free-moving mice. The temperature-controlled animal chamber (left panel) and the inside of the chamber (middle panel), in which four mice can be recorded at once, are shown. Each animal had an intraperitoneally implanted body-temperature transmitter (right panel, top). Each animal was housed in a metabolic chamber and the VO_2 were recorded by gas mass spectrometry. (c) A representative recording of mouse metabolism for three consecutive days. The animal was placed in the chamber, and the T_A was maintained at 16 °C. Once the mouse was placed in the metabolic chamber, there was no physical contact with researchers during the recording period. Note the clear circadian rhythm seen in the T_B , VO_2 and locomotion. Yellow shading shows the light-on period. (d) A representative recording of metabolism during fasting-induced daily torpor. The mouse was placed in the chamber for three days; food was removed on the second day (filled triangle). The T_A was maintained at 16 °C. Daily torpor started during the latter half of the second day. The mouse returned to a euthermic state immediately after the food was returned to the chamber (unfilled triangle). Yellow shading shows the light-on period.

secondary trend, to be 0.01877 and 0.00650 for T_B and VO_2 , respectively (Fig. 2e). By fixing σ_2 to these values, our model can estimate the animal's individual baseline T_B and VO_2 dynamics from data taken over a single day rather than from multiple periods. This method effectively shortens the baseline recording period and lowers the stress on the animal. To verify the quality of the model, we estimated the baseline metabolism dynamics in another set of animals ($n=4$, $T_A=16$ °C, mice 9 to 12) by applying these σ_2 values (Fig. 2f and Supplementary Fig. 2c). More than 99% of the sampling points on the second and third day were included in the 99.9% credible interval (CI) of both the estimated T_B and VO_2 (Fig. 2g). Therefore, for each subject, the first day's recording was sufficient to predict the dynamics of T_B and VO_2 for the following two days. In the following analysis, a 99.9% CI was applied for estimating the baseline distribution for T_B and VO_2 , respectively. Development of this simple but individualized metabolism modelling allowed us to define daily torpor as an outlier from the individually predicted baseline dynamics of metabolism.

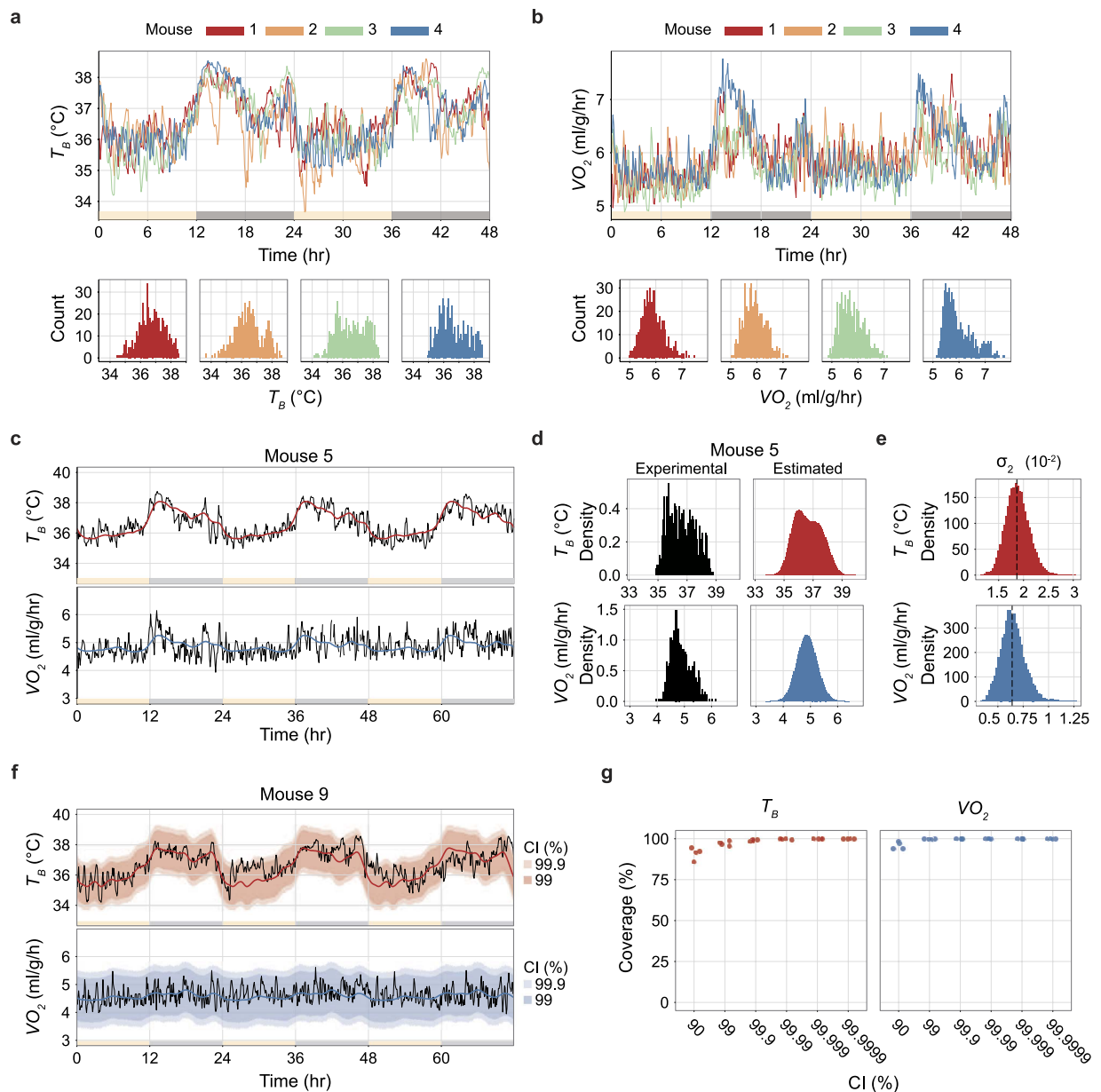


Figure 2. Modelling and predicting metabolism from a single day recording. (a,b) The distribution of the T_B (a) and VO_2 (b) of four animals (mice 1 to 4) kept at a T_A of 12°C for two days. The upper panels show the time series; light and dark periods are indicated by yellow and grey bars along the horizontal axis. The distribution for each animal is shown in the lower panels; each colour represents a different animal. (c) The estimated baseline metabolism dynamics of mouse 5. The mouse was kept at a T_A of 16°C for three days. The baseline dynamics for 24 hours were fitted from the three-day-length data, and the standard deviation of the error (σ_2) for both T_B and VO_2 was estimated. The red and blue lines denote the median of the posterior distribution of the estimated T_B and VO_2 , respectively. The data for the remaining three animals (mice 6 to 8) are available in Supplementary Fig. 2a. (d) The probability density of the experimentally obtained and estimated data for T_B and VO_2 for mouse 5. Black histograms represent experimental data; red and blue histograms show the estimated probability density. The data for mice 6 to 8 are available in Supplementary Fig. 2b. (e) The distribution of the estimated σ_2 , which is the standard deviation of the error of the secondary trend, for T_B and VO_2 . (f) The estimated baseline metabolism dynamics of mouse 9 with credible intervals (CIs). The T_A was kept at 16°C for three days. The first 24 hours were used for estimation. The red and blue lines denote the median of the posterior distribution of the estimated T_B and VO_2 . The red and blue shaded areas denote the CI. The data for mice 10 to 12 are available in Supplementary Fig. 2c. (g) CI coverage rate of the metabolism on the second and third days when applying different CI ratios. The estimation was based on the first day. For both T_B and VO_2 , 99.9% of the CIs covered more than 99% of the sampling points of the latter two days.

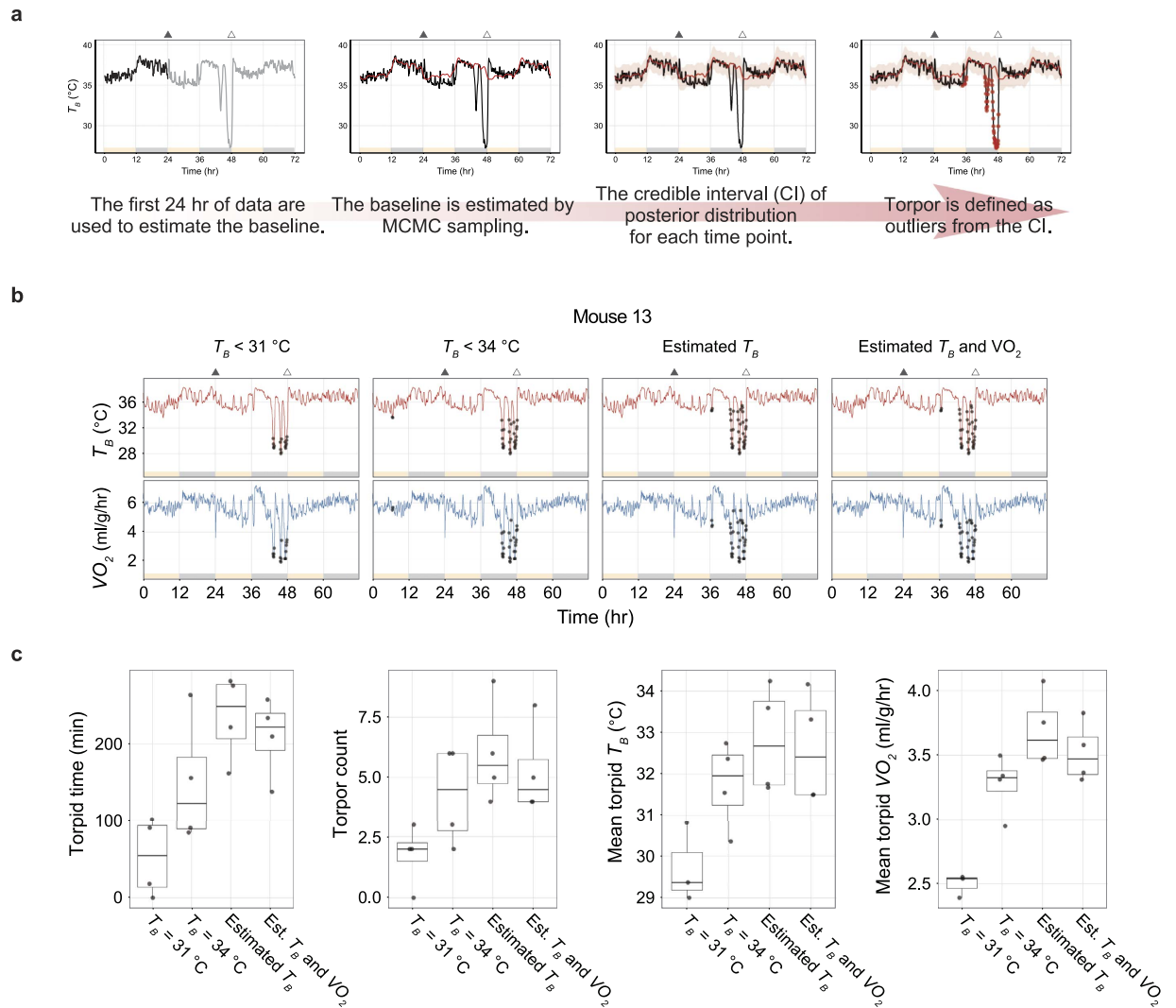


Figure 3. Defining daily torpor as an outlying low metabolism. (a) The daily torpor-detection pipeline. The first 24-hour data set is used to estimate the baseline metabolism of the individual animal (first panel). The estimated baseline is then applied to the rest of the recordings (second panel). The baseline estimation provides the CI for the prediction from the distribution of the posterior estimates (third panel). Torpor, which is defined as a lower outlier from the CI, is marked in red dots (fourth panel). The filled and unfilled triangles denote food removal and return, respectively. (b) Multiple torpor definitions were compared in four mice (mice 13 to 16). The animals were placed in a constant T_A of $12\text{ }^{\circ}\text{C}$ for three days, and food was restricted during the second day. Results are shown for mouse 13. The two leftmost panels show daily torpor defined by a fixed threshold T_B of $31\text{ }^{\circ}\text{C}$ or $34\text{ }^{\circ}\text{C}$. The third panel shows daily torpor defined by a lower outlier of the 99.9% CI of the estimated T_B . The fourth panel includes the T_B -based definition further narrowed down by adding the condition of lower outliers from the 99.9% CI of the estimated VO_2 . The filled and unfilled triangles denote food removal and return, respectively. The data for the remaining three animals are available in Supplementary Fig. 3a. (c) Boxplots for various torpor statistics according to the different torpor definitions listed in Fig. 3b. The band inside the box, the bottom of the box, and the top of the box represent the median, the first quartile, and the third quartile, respectively. The end of the upper whisker is the highest value that is within 1.5 times the interquartile range (IQR). The end of the lower whisker is the lowest value that is within 1.5 times the IQR. All data points are shown as grey dots.

Defining daily torpor as an outlying low metabolism. Because daily torpor is a state in which animals show abnormally low metabolism, it is reasonable to define daily torpor as an outlier from the baseline metabolism. Using the statistically estimated baseline metabolism, we defined daily torpor when both T_B and VO_2 were lower than the 99.9% CI of the prediction (Fig. 3a). To evaluate the functionality of this new approach, we conducted another experiments in four mice ($n = 4$, $T_A = 12\text{ }^{\circ}\text{C}$, mice 13 to 16). We found that conventional methods^{10,22} detected lower rates of torpor than our method (Fig. 3b,c and Supplementary Fig. 3a). Our novel approach allowed us to objectively quantify the length and depth of daily torpor by normalizing the variance among individual recordings. Although there was little discrepancy between torpor definitions using only T_B or T_B and VO_2 (Fig. 3c), torpor defined from VO_2 alone detected a higher rate of torpid status in the current study

(Supplementary Fig. 3b). Applying this simple but robust torpor-detection method, we next investigated how T_A influences metabolism during daily torpor. The comprehensive analysis of T_A dependent phenotype of daily torpor allowed us to estimate the fundamental factors of thermoregulatory system during torpor.

Body-temperature homeostasis is actively controlled during torpor. A constant body temperature is a key characteristic of mammals. The thermoregulatory system is apparently altered during daily torpor, because the T_B is lower than in normal states. To test the influence of T_A on T_B during daily torpor, we kept the animal under a constant T_A of 8, 12, 16, 20, or 24 °C and removed food for 24 hours to induce daily torpor (Fig. 4a and Supplementary Fig. 4a). The minimal metabolic point was defined at a point where the T_B is minimized within the time-range of interest.

To model the temperature dependent metabolism, first, we linearly regressed minimal VO_2 and T_B with T_A during the second-half of Day 1 as follows:

$$T_B = a_1 T_A + b_1 \quad (1)$$

$$VO_2 = -a_2 T_A + b_2 \quad (2)$$

According to the estimation, the minimum T_B remained nearly constant against changes in T_A , as the 89% highest posterior density interval (HPDI) of the slope a_1 was between 0.024 and 0.063 and the mean was 0.043 (Fig. 4b,c, red lines) while the minimal VO_2 during non-torpid status was negatively correlated with the T_A and the 89% HPDI of the a_2 was between 0.188 and 0.216 ml/g/hr/°C and the mean was 0.203 ml/g/hr/°C (Fig. 4d,e, red lines).

We next analyzed the torpor-inducing efficiency of removing food for 24 hours. When the T_A was 12 °C or higher, 100% of the animals tested entered daily torpor, while when the T_A was lowered to 8 °C, only 54.5% of the animals succeeded to enter torpor (Fig. 4f). Although the T_A did not affect the frequency of animals entering torpor during a fasting episode (Supplementary Fig. 4b), the total duration of daily torpor tended to prolong with lower T_A (Supplementary Fig. 4c). Interestingly, this tendency was held even in comparing the average duration of a single period of daily torpor (Fig. 4g).

Moreover, we evaluated the metabolism of the animal during daily torpor. When T_A was higher than 12 °C, T_B decreased dramatically (Fig. 4b, blue lines) during torpor. For example, at $T_A = 12$ °C, minimal T_B reduced from 35.4 ± 0.17 °C to 27.4 ± 0.88 °C during torpor (mean \pm SEM, $n = 8$). This is completely different from the normal state, in which the T_B hardly changed at around 36 °C (Fig. 4b). Furthermore, the fact that a_1 increased 5.9 times from the normal status (89% HPDI of the a_1 was between 0.147 and 0.365, the mean was 0.257, Fig. 4c) indicated that T_A strongly influences T_B during daily torpor. VO_2 also decreased prominently during daily torpor. At $T_A = 12$ °C, the drop of VO_2 was $46.6 \pm 4.0\%$ (mean \pm SEM, $n = 8$, Supplementary Fig. 4d). In contrast to T_B , the minimal VO_2 during torpor became less sensitive to T_A , which is clearly shown by the decrease of a_2 (89% HPDI was between 0.085 and 0.121 ml/g/hr/°C, the mean was 0.103 ml/g/hr/°C, Fig. 4d,e). These results indicate the thermoregulation mechanism during daily torpor was weakened. As a result, T_B becomes sensitive to T_A . However, the active thermoregulation was not completely abolished. When we further lowered the T_A to 8 °C, the mean minimal T_B and VO_2 during torpor were 27.6 °C and 2.83 ml/g/hr ($n = 6$), respectively. Both of these values were higher than the upper end of 89% HPDI of the estimated mean (Fig. 4h,i) suggesting that at $T_A = 8$ °C, an additional thermoregulatory mechanism has been kicked in. This was not apparent when T_A was at the range of 12 to 24 °C.

Finally, to evaluate the extent of active reduction of metabolism during daily torpor, we calculated the Q_{10} temperature coefficient of VO_2 with T_B during torpor. Surprisingly, Q_{10} was as high as 6.39 at $T_A = 24$ °C, decreased along with the lowered T_A and reached to 3.12 at $T_A = 12$ °C. Because Q_{10} was greater than 3, the reduction of VO_2 cannot be explained solely by the effect of hypothermia, implicating that the metabolism was actively decreased resulting in hypothermia.

Overall, these results demonstrate that the metabolic regulation for homeostatic control of the T_B is weakened during daily torpor, and T_B changes nearly passively with T_A . The thermoregulatory system is further altered when the T_A drops to 8 °C, implying the existence of a secondary mechanism that remains active to keep the metabolism at a certain level even during daily torpor, reminiscent of the hibernators. To estimate the target components of thermoregulation during daily torpor, we next fitted the data to a mathematical model to estimate the parameters of the thermoregulatory system. This analysis revealed a difference between daily torpor and hibernation thermoregulation.

The sensitivity of the heat production system is largely reduced during daily torpor while the reduction of set-point temperature is small. From the experimental results in our study, we found that the thermoregulatory system during daily torpor has dynamic properties over the T_A (Fig. 4b–d). To elucidate the main effectors of this dynamic system, we have fitted the results to the thermoregulation model consisting of a heat production and heat loss loop (Fig. 1a).

This model describes the thermoregulatory feedback system of the animal when the animal is not moving. The energy lost from the animal (Q_{out}) is thermodynamically determined by the difference of T_B from T_A and the heat conductance (G) of the animal. The metabolic rate (Q_{in}) is the energy used for heat production per unit time and it is designed to be a function of the difference of T_R from T_B . In this study, for simplicity, we expressed both Q_{in} and Q_{out} as oxygen consumption rates (O_2 ml/g/hr) and assumed the measured VO_2 is equals Q_{in} . This is possible when the energy production is proportional to VO_2 . The net change in heat, i.e. $Q_{in} - Q_{out}$, divided by heat capacity C yields the time derivative of T_B as:

$$\frac{Q_{in} - Q_{out}}{C} = \frac{d}{dt} T_B \quad (3)$$

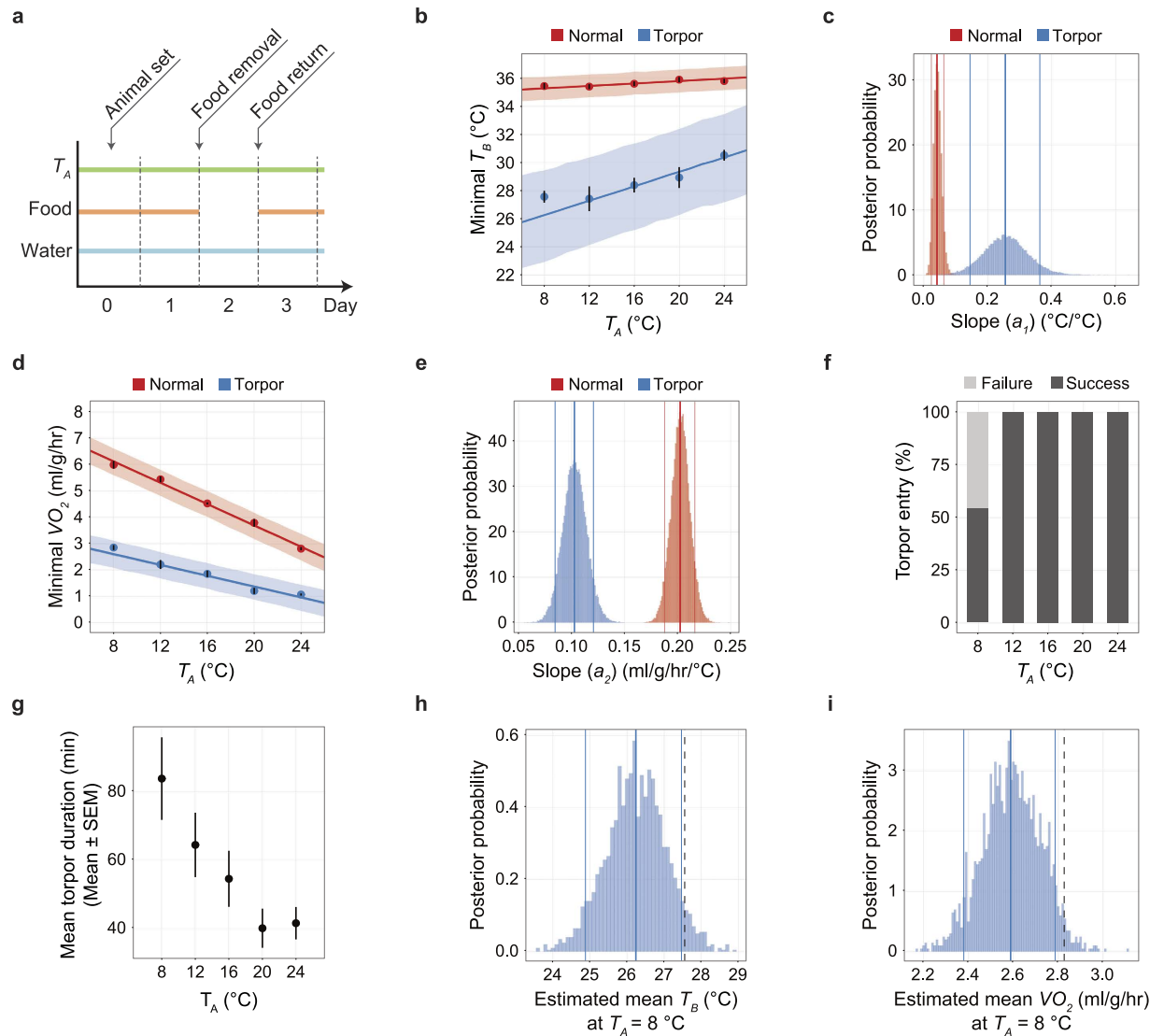


Figure 4. Body-temperature homeostasis is actively controlled during daily torpor. (a) Protocol of the fasting-induced daily torpor experiment. Animals were placed in the T_A -constant chamber on Day 0; data were recorded for 72 hours from the beginning of Day 1. Food was removed and returned at the beginning of Day 2 and Day 3. Water was freely accessible throughout the experiment. (b) The minimum T_B at various T_A s. Including the following panels, red and blue denote normal and torpid status, respectively. For normal status, the minimum T_B of the dark phase of Day 1 was used for analysis. For torpid status, the minimum T_B during torpor was used for analysis. As in the following panel d, the dots with the vertical error bars denote the observed mean and SEM of the minimum variables (T_B in b, VO_2 in d) at each T_A , and the line and the shaded area denote the mean and the 89% HPDI intervals of the estimated minimum variables. (c) The posterior distribution of the slope (a_1) of T_A - T_B relationship. Including the following distribution panels in this figure, the bold and thin lines denote the mean and the 89% HPDI intervals of the estimated values. The bin size is 0.005. (d) The minimum VO_2 at various T_A s. Minimum VO_2 was defined as the VO_2 recorded when the T_B was minimum. (e) The posterior distribution of the slope (a_2) of T_A - VO_2 relationship. The bin size is 0.001 ml/g/hr/ $^\circ\text{C}$. (f) The rate of successful daily torpor induction at various T_A s. When T_A was above 12°C , all animals entered daily torpor. (g) The averaged torpor duration for each episode. One torpor episode is tended to be shorter when the T_A gets higher. (h, i) The posterior distribution of the estimated mean ($n = 6$) of T_B (h) and VO_2 (i) at a T_A of 8°C . Because the observed mean (dashed lines) is larger than the 89% HPDI in both T_B and VO_2 , when $T_A = 8^\circ\text{C}$, the animal exhibited higher metabolism than expected. The bin size is 0.1°C and 0.01 ml/g/hr for T_B and VO_2 , respectively.

In the heat loss loop (the upper loop in Fig. 1a), if the animal is not moving, because no energy is used for external work by exercise, the Q_{out} from the animal is mainly governed by the difference of T_B and T_A as:

$$Q_{out} = (T_B - T_A)G \quad (4)$$

Furthermore, if T_B is in the steady-state (i.e., $dT_B/dt=0$), Q_{out} equals Q_{in} from equation (3). Substituting Q_{out} in equation (4) with VO_2 yields:

$$VO_2 = (T_B - T_A)G \quad (5)$$

This means all of the oxygen consumption is utilized for heat production to fill the gap between the body and ambient temperature.

On the other hand, in the heat production loop (the lower loop in Fig. 1a), if the animal is still, Q_{in} is proportional to the difference between the set-point temperature T_R and T_B as:

$$Q_{in} = (T_R - T_B)H \quad (6)$$

Under the steady-state condition, equation (6) can be rewritten as:

$$VO_2 = (T_R - T_B)H \quad (7)$$

Eliminating VO_2 by joining equations (5) and (7), under the steady-state condition, T_B can be described as:

$$T_B = \frac{H}{G+H}T_R + \frac{G}{G+H}T_A \quad (8)$$

In this model, three parameters are modifiable by the body. One is the heat conductance (G), which is the main parameter quantifying the heat loss of the animal, and the other two are the body temperature set-point (T_R) and the gain of the negative feedback loop of heat production (H). Because not all animals enter torpor when $T_A = 8^\circ\text{C}$ (Fig. 4f), we employed T_B and VO_2 recorded under $T_A = 12, 16, 20$ and 24°C for the parameter estimation.

First, we estimated G from equation (5) by fitting experimental data (Fig. 5a). We found that G decreased from 0.228 to 0.144 ml/g/hr/ $^\circ\text{C}$ during daily torpor (Fig. 5b). The 89% HPDI was 0.224 to 0.231 ml/g/hr/ $^\circ\text{C}$ and 0.137 to 0.151 ml/g/hr/ $^\circ\text{C}$ for normal and torpid status, respectively. The decrease of G reduces heat loss by 37% during daily torpor, thereby serves as a mechanism of heat preservation. Therefore, the decreased G counteracts to the reduction of T_B and necessitates even more profound hypometabolism to lower T_B during daily torpor.

Next, we estimated T_R and H from equation (7). Because we have estimated the relationship of T_B and VO_2 with T_A from equations (1) and (2) in the previous section, we used those results to further estimate T_R and H . Eliminating T_A from equations (1) and (2) results in:

$$VO_2 = \left(\frac{a_2 b_1 + a_1 b_2}{a_2} - T_B \right) \frac{a_2}{a_1} \quad (9)$$

From equations (7) and (9), both T_R and H can be described by a_1, a_2, b_1 and b_2 as:

$$T_R = \frac{a_2 b_1 + a_1 b_2}{a_2} \quad (10)$$

$$H = \frac{a_2}{a_1} \quad (11)$$

Applying the estimated a_1, a_2, b_1 and b_2 (Fig. 4c,e and Supplementary Fig. 5a,b), we obtain T_R and H . Figure 5c represents the estimated T_B - VO_2 relationship with the observed data. In this figure, the horizontal intercept denotes the T_R , because theoretically the thermoregulatory system will no longer produce heat when the T_B equals T_R . In normal status, the 89% HPDI of the estimated T_R was between 36.1 and 37.2 $^\circ\text{C}$ (Fig. 5d, red histogram). Interestingly, during torpor, the 89% HPDI of T_R was estimated to be between 30.9 and 34.7 $^\circ\text{C}$ (Fig. 5d, blue histogram). These are lower than in normal status but not as low as the observed T_B during torpor (Fig. 4b). These results clearly showed that the hypometabolism during daily torpor cannot be explained only by a low T_R . In fact, the gain of the negative feedback loop of heat production (H), which is represented by the negative slopes of the lines in Fig. 4c during normal and torpid status turned out to be very contrasting. The 89% HDPI of the estimated H during normal status was between 2.79 and 7.36 ml/g/hr/ $^\circ\text{C}$ (Fig. 5e, red histogram), while during torpor, it decreased to values between 0.233 and 0.624 ml/g/hr/ $^\circ\text{C}$ (Fig. 5e, blue histogram). The averaged estimated H of torpid status showed 91.5% reduction from the normal status. Overall, we conclude that the striking reduction in the open-loop negative feedback gain of the heat production system plays the central role in regulating the hypometabolism during daily torpor. The contributions of a small reduction of T_R and G are secondary.

Discussion

Metabolism during daily torpor is actively regulated to stay above a certain level. We developed a simple but robust method to estimate the individualized baseline metabolism of mice and defined daily torpor as an outlier of the baseline metabolism (Figs 1, 2 and 3). Since the baseline is defined from the animals in *ad libitum* access to food (day 1), the abnormal low metabolism detected in our study may include the metabolic drop caused by fasting itself. This may be a problem to discriminate the fasting response and the torpid response to evaluate what extent the torpor time is influenced by fasting. However, our main aim to apply the baseline metabolism is to absorb the individual variance in metabolism. Therefore, we defined daily torpor of an animal by including the fasting response as a part of the hypometabolic response.

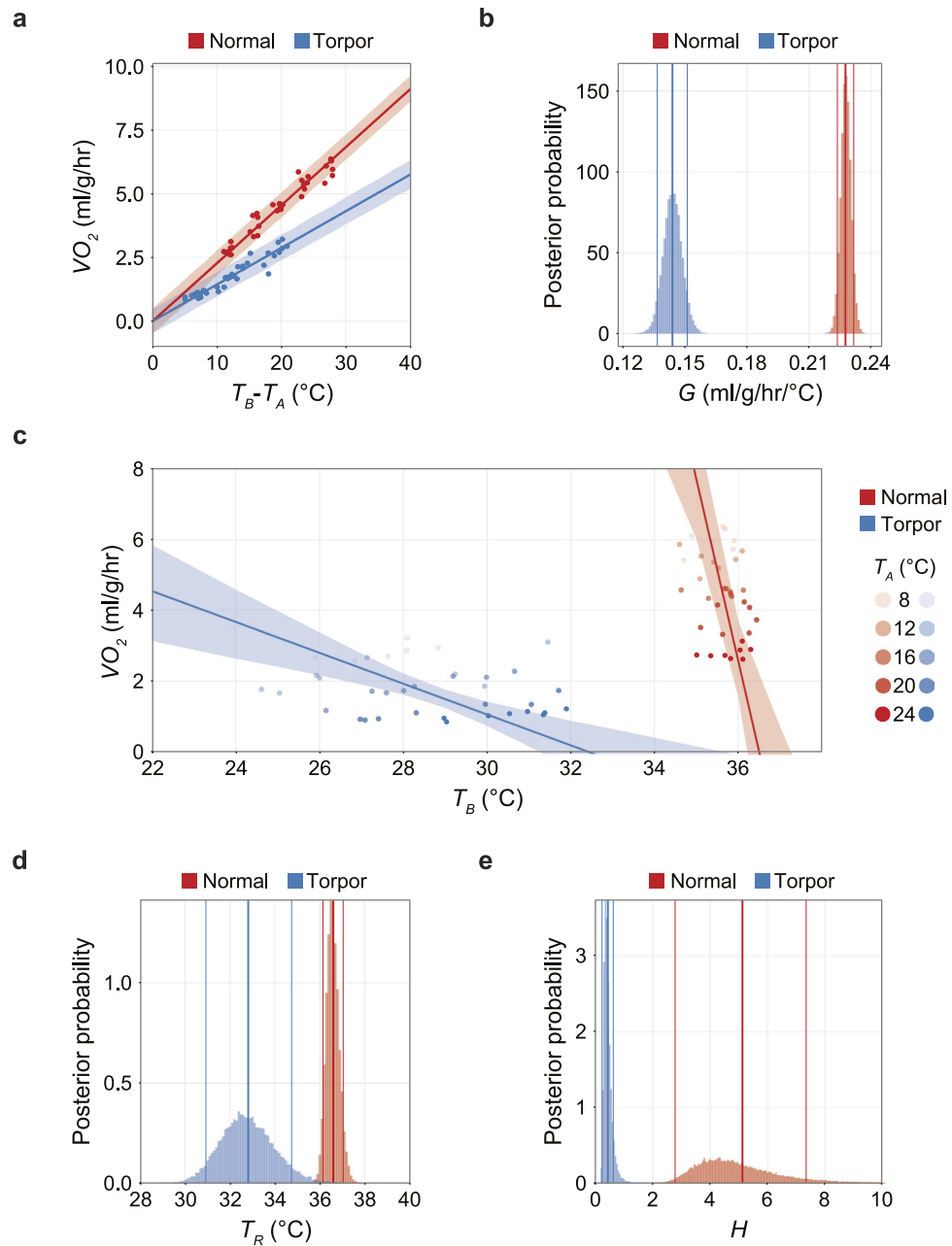


Figure 5. The sensitivity of the heat production system is largely reduced during daily torpor while the reduction of set-point temperature was small. (a) The relationship between the difference of T_B from T_A and VO_2 . Including the following panels, red and blue denote normal and torpid status, respectively. The slope of this relationship is the heat conductance, G . As in panel c, the dots represent the observed values, and the lines and shaded areas represent the means and the 89% HPDI intervals of the estimated values. (b) The posterior distribution of the estimated G . During torpor, G is smaller than during normal states. Decrease in G results in heat preservation. However, the T_B decrease seen in daily torpor is indicating the decrease in G is overridden or induced by decrease of heat production. The bin size is 0.001 ml/g/hr/°C. As in panel d and e, the bold and thin lines denote the mean and the 89% HPDI intervals of the estimated values. (c) The relationship between minimum T_B and VO_2 seen during normal and torpid states among various T_A s. The brightness of the dots is indicating the T_A . The horizontal intercept of the line indicates the theoretical set-point of T_B , which is T_R (See Fig. 1a). During normal states, T_B is kept relatively constant by employing oxygen and producing heat to fill the gap between T_R and T_A . On the other hand, during daily torpor, the sensitivity against $T_R - T_B$ is weakened which is visualized by less steep slope, which is H , the open-loop negative feedback gain of the heat production loop (See Fig. 1a). (d) The posterior distribution of the estimated T_R . During daily torpor, T_R became smaller than normal states, although the mean difference was 3.79 °C. The bin size is 0.1 °C. (e) The posterior distribution of the estimated H . During daily torpor, H became dramatically smaller than normal states, which the mean difference reached to 4.70 ml/g/hr/°C. This is clearly showing that the open-loop gain of the heat production system reduced to 8.5% during daily torpor from the normal state. The bin size is 0.05 ml/g/hr/°C.

We showed that during daily torpor, the metabolism is dynamically regulated in response to changes in T_A . In torpid periods when T_A was 12 °C or higher, the T_B responded nearly passively to T_A (Fig. 4d) in a semi-heterothermic manner. Notably, when the T_A dropped to 8 °C, the animals stopped responding semi-heterothermically and the minimum T_B and VO_2 were higher than they were predicted (Fig. 4h,i).

Interestingly, the minimum T_B reported during daily torpor varies among studies^{10,21,24,25}. The minimum T_B during daily torpor strongly correlated with T_A . Therefore it is possible that our observed minimum T_B was higher than in other studies because of differences in T_A . However, since we measured the minimum T_B for a wide range of T_A (8 to 24 °C), it is unlikely that the differences in the minimum T_B are due to T_A variance. Other factors, such as genetic differences in the animals used in the study must be considered. Indeed, differences in daily torpor phenotype have been reported among inbred strains¹⁸. Therefore, tracking the minimum T_B phenotype among genetically modified or genetically distinct mice, such as genetically knockout animals or other inbred strains, may contribute to our understanding of the resistance to hypothermia, which is one of the four major requirements for active hypometabolism capability.

In addition, the phenomenon of the animal returning to a homeothermic state when the T_A drops below a certain level is seen not only in daily torpor, but also during hibernation¹³. This suggests that a common mechanism underlies both daily torpor and hibernation, and that studying torpor in mice may help to reveal a universal mechanism of active hypometabolism.

Finally, it is worth noting that the oscillative behavior of metabolism during torpor was always seen in our study. This is discrepant from previous studies which typically show continuous lowered levels of VO_2 or T_B ^{10,26}. We think the oscillatory metabolism during torpor is partially because the animals we have used are exclusively males. We decided to use male rather than female to avoid the possible reproductive cycle effect, which are often seen in sleep/wake cycles^{27,28}. If the sex difference in torpor phenotype is globally observed through *Mus musculus*, it may be a good lead to investigate the dynamic change of the thermoregulatory parameters during daily torpor.

The active thermoregulation during daily torpor is mainly driven by less sensitivity of the heat production system. In this study, estimating G , T_R and H from observations of T_B and VO_2 among various T_A s, we concluded that the reduction in H is the main effector of hypometabolism during daily torpor (Fig. 1a and 5c). Importantly, equation (8) shows the ratio of G and H determines the contribution of T_R and T_A to T_B . When $G > H$, the T_A has stronger effect to T_B , and when $H > G$, the T_R has stronger effect to T_B . In this study, G/H increased from 0.044 to 0.330 when the animal entered torpor. This is clearly showing that during daily torpor, the thermoregulatory system shifted to accept the effect of T_A and as a result, the effect of T_R had been relatively weakened.

We observed the decrease in G in torpid mouse as it was reported in past literatures and in other species¹². This will decrease the heat loss, which can be explained as the secondary effect of low T_B against T_R . The reaction to decrease heat loss is also supported by the torpor specific statue observed in this study (Supplementary Movie 3) that can be the result of minimizing the surface area to reduce heat loss. The slight drop in T_R is indicating that its contribution to torpor thermoregulation is insignificant to the decrease in H (Fig. 5b,d,e). This is fundamentally different from hibernators which usually show reduction not only in H but also in T_R ^{8,9,17}. However, the degree of reduction of H during daily torpor was similar to that of hibernators. This is indicating that the sensitivity reduction in thermogenesis in daily torpor may share a common mechanism with hibernation.

For example, Yellow-bellied marmots (*Marmota flaviventris*) have $T_R = 36.3\text{--}37.0$ °C and $H = 0.136\text{--}0.253$ ml/g/hr/°C during euthermic states⁹. During hibernation, T_R drops to 6.2–9.5 °C and H decreases to 0.006–0.023 ml/g/hr/°C which is nearly a 90% decrease. Importantly, both T_R and H are reduced. Another example is seen in golden-mantled ground squirrels (*Citellus lateralis*), which reduce T_R from 37.2–37.9 to 1.2–12.5 °C during hibernation^{8,17}. In these species, H is reduced from 0.781–1.20 to 0.032–0.073 ml/g/hr/°C which is more than a 90% reduction.

There are, at least, three possible explanations for dominantly lowering H but not T_R during daily torpor. One is based on structure of the thermoregulatory system (Fig. 1a). It is possible to control T_B by changing both T_R and H , as in hibernators. However, regulating multiple actuators is much complicated than controlling a single actuators, and as a system, usually it is easier to obtain stability when the number of actuator is less. Moreover, since daily torpor is only induced for hours, where hibernators stay in hypometabolic states for days, it is reasonable to keep the regulatory system during torpor simpler and much controllable than in hibernation. The drawback of keeping the T_R high is the higher T_B . As in equation (8), when having G and H at the level as low as hibernators with a fixed T_A , T_B depends on T_R . For hibernators, which have to survive for several months without eating, lowering the T_R along with H is reasonable.

The second possible reason for not lowering T_R during daily torpor rises from one of the requirements for a mammal to enter active hypometabolism, the resistance to hypothermia. Even during daily torpor, the animal will appreciate as low metabolism as possible if the aim of the hypometabolism is to save energy. Therefore, leaving T_R in a relatively high value indicate there is a minimum temperature the animal can accept. Indeed, the torpid animals showed higher metabolism than expected from the trend when T_A was lowered to 8 °C (Fig. 4h,i).

The third possible explanation can also be derived from another requirement for mammalian active hypometabolism, the rewarming function from hypometabolic state. Hypometabolic animals have to produce heat to return to euthermic condition. Hibernation and daily torpor exhibit different time-courses during the rewarming. In hibernators, they return to euthermic condition within hours, while in daily torpor, animals rewarm in less than an hour (Fig. 3b and Supplementary Fig. 3a). It is well documented that in hibernators, the decrease of T_R takes longer time than decrease of H ⁹. The slower dynamics of T_R regulation imply a certain underlying mechanism to prevent the T_R to decrease as quick as H . Because T_R is regulated in the brain, it is natural to assume the

T_R is controlled through the dynamic change in the neural network such as synaptic plasticity, which may require considerable energy and time in either increasing or decreasing T_R . Therefore, in daily torpor, to implement a minute-order rewarming, changing the T_R would be nothing but a hurdle, which can be a possible reason why it is not lowered as in hibernators.

Our results clearly show that the reduction in the open-loop gain of the thermogenesis system, which is the sensitivity to the temperature gradient between T_B and T_R , is the major effector of hypometabolism in mouse daily torpor. Throughout the thermosensory afferent and the thermogenesis efferent pathway²⁹, theoretically, suppressing any of the sites can reduce the feedback gain. Basically, they can be grouped into central or peripheral mechanisms according to the suppressed site. In the central nervous system (CNS), it is possible that the preoptic area in the brain, including the thermoregulatory centre, is sending fewer signals to produce heat. If this is the case, there should be less neural activity at the thermoregulatory centre or at upstream of that. On the other hand, it is possible that even though the brain is sending signals to produce heat, the peripheral tissue (i.e. brown adipose tissue or skeletal muscle) may not be producing heat because it does not receive the signal properly or is unable to respond to the signal. Either scenario can reduce H without altering the set-point temperature. While alternation in thermoregulatory system is another requirement for the capability to undergo active hypometabolism, further investigation is necessary to narrow down the mechanism of reduced H in daily torpor.

One approach to investigate the thermoregulatory modification in the CNS is to utilize the novel imaging technology to evaluate the CNS systematically during daily torpor^{30,31}. Determining whether specific parts of the brain, including the thermoregulatory centre, are active or inactive during daily torpor will provide important clues to how the regulatory network of hypometabolism functions. The other approach is to examine the peripheral tissue during torpor. As in the present study, the overall reduction of the animal's metabolism can be evaluated by analysing the VO_2 from respiration. However, the variations in hypometabolism among organs and tissues can only be evaluated by testing the metabolism in each component. Because the basic metabolic rate varies among organs and tissues during euthermia, the reduction in metabolic rate may also differ among organs and tissues during hypometabolism. Investigating the localization of hypometabolism during daily torpor will offer new insights into the regulatory mechanism of active hypometabolism and may also offer clues to the mechanism by which the animal rewarms from a very hypometabolic state, which is another requirement for an animal to safely enter a hypometabolic state.

Toward active hypometabolism implementation in humans. Humans may benefit from active hypometabolism. In stroke, it is important to begin treatment as quickly after the onset of symptoms as possible³² because outcomes worsen as time passes due to hypoxia of the brain. If we could reduce the demand for oxygen by inducing active hypometabolism, the patient could buy time by slowing the progress of brain damage and thus may survive periods of hypooxygenation.

Tissue and organ preservation can also benefit from induced hypometabolism. Regenerative therapies have been approved for selected organs (Mandai *et al.*, in preparation), and clinical studies are underway for others. One of the inherent problems in this field is how to preserve tissues or organs once produced, keeping them healthy and fresh. Cooling is currently a mainstay for preserving organs, but cannot keep organs alive for weeks. Rather than removing heat, reducing the metabolism by active hypometabolism may solve this problem. Torpid animals do not have low metabolism because they are cold; they are cold because they have low metabolism.

To implement active hypometabolism in humans, we need to deal with the four conditions, which were mentioned in the Introduction. Recently, several species of primates were found to be hibernators^{33,34}. Although it is tempting to investigate hypometabolism in an animal that is close to humans, monkeys are difficult to use due to their limited availability. Non-primate hibernators are alternative candidates for understanding the mechanism of hypometabolism but the seasonal effect of the hypometabolism is a burden for aggressive research. Therefore, we think mouse is an ideal animal to investigate hypometabolism for future clinical application. Thus, this study has great importance as a pioneering and fundamental work to clarify the mechanism of active hypometabolism in mouse, and moreover, for the development of the next generation hypometabolic medicine.

Methods

Animal experiments. All animal experiments were performed according to the guidelines for animal experiments of RIKEN Center for Developmental Biology and approved by the Animal Experiment Committee of the RIKEN Kobe Institute (Approval ID: AH27-05-4). C57BL/6Njcl mice were purchased from CLEA Japan, Inc. and C57BL/6J mice were from Oriental Yeast Co., Ltd. Until the mice were used in torpor experiments, they were given food and water *ad libitum* and maintained in an ambient temperature of 21 °C, a relative humidity of 50%, and a 12-hr light/12-hr dark cycle.

Two C57BL/6Njcl male mice were used for the experiments shown in Fig. 1c,d; 57 C57BL/6J male mice were used for the rest of the experiments. The age at the time of the experiment was 8.01 ± 0.15 weeks (mean \pm SD, $n = 59$).

During the experiments, each animal was housed in a temperature-controlled chamber (HC-100, Shin Factory), and the temperature inside the chamber was monitored continuously by a temperature logger (Thermochron iButton, DS1922L-F5#, Embedded Data Systems). To record T_B continuously, a telemetry temperature sensor (TA11TA-F10, DSI) was implanted in the animal's abdominal cavity under general inhalation anaesthesia at least 7 days before recording. The metabolism of the animal was continuously analyzed by respiratory gas analysis (ARCO-2000 mass spectrometer, ARCO system). During the experiment, the animal was monitored through a network video camera (TS-WPTCAM, I-O DATA, Inc.) and movies were recorded as needed. This video camera's ability to record infrared movies made it possible to monitor the animal's health during the dark phase without opening the chamber.

Body temperature and oxygen consumption modelling with daily torpor detection. To model the temporal variation of T_B and VO_2 , we constructed the models in a Bayesian framework and estimated the parameters using Markov Chain Monte Carlo (MCMC) sampling by Stan³⁵ with the RStan library³⁶ in R³⁷. The fundamental principles and techniques for designing the model were based on the book *Statistical Rethinking*³⁸.

When the unobservable baseline of T_B or VO_2 is defined as a time-variable α_k , with the noise factor ε_t , the total time point in a day K , and the total number of days in the time series D , the observed state Y_t can be described as:

$$Y_t = \alpha_k + \varepsilon_t \quad (12)$$

$$\varepsilon_t \sim \text{Normal}(0, \sigma_1^2) \quad (13)$$

$$t = k + K \cdot d \quad (14)$$

$$d = 1 \cdots D \quad (15)$$

$$k = 1 \cdots K \quad (16)$$

α_i is defined in a circulatory secondary trend model as

$$\begin{cases} \alpha_1 - \alpha_K = \alpha_K - \alpha_{K-1} + \eta_1, & k = 1 \\ \alpha_2 - \alpha_1 = \alpha_1 - \alpha_K + \eta_2, & k = 2 \\ \alpha_k - \alpha_{k-1} = \alpha_{k-1} - \alpha_{k-2} + \eta_k, & k \geq 3 \end{cases} \quad (17)$$

$$\eta_k \sim \text{Normal}(0, \sigma_2^2) \quad (18)$$

$$k = 1 \cdots K \quad (19)$$

Equation (17) can be transformed as:

$$\begin{cases} \alpha_1 = 2\alpha_K - \alpha_{K-1} + \eta_1, & k = 1 \\ \alpha_2 = 2\alpha_1 - \alpha_K + \eta_2, & k = 2 \\ \alpha_k = 2\alpha_{k-1} - \alpha_{k-2} + \eta_k, & k \geq 3 \end{cases} \quad (20)$$

Using three-day recordings of metabolic data from four non-torpid mice, we estimated the posterior distribution of the σ_2 of both T_B and VO_2 by MCMC sampling of the equations (12) to (20) (Fig. 2c and Supplementary Fig. 2a). Uniform priors were applied for every parameter. We fixed the σ_2 to the median of the posterior distribution (Fig. 2e), and using another four animals, we estimated α_k from a single-day-length recording for each animal and calculated the posterior distribution of Y_t (Supplementary Source Code 2). We calculated the minimum interval of Y_t that can predict the metabolic dynamics shown in Fig. 2f and Supplementary Fig. 2c. In the remaining analyses, we used the 99.9% CI of the posterior distribution of Y_t estimated from the animal's first day of recordings to detect outliers. That is, when the value was lower than the CI, that time point was defined as torpor due to an abnormally low metabolic status (Fig. 3a). In this study, when both T_B and VO_2 met the criteria, the time point was treated as torpor.

Daily torpor induction experiment. Each daily torpor induction experiment was designed to record the animal's metabolism for three days (Fig. 4a). The animals were introduced to the chamber the day before recording started (Day 0). Food was placed on the floor, and a water bottle was made available. The thermosensor implanted in the mouse was turned on before placing the mouse in the chamber. We began recording metabolic data at the beginning of the light phase, which was ZT-0 of Day 1. On Day 2, ZT-0, the food was removed to induce torpor. After 24 hours, on Day 3, ZT-0, the food was returned to each animal.

Parameter estimation of the thermoregulatory system. To thermoregulatory system was modelled as an integration of the heat loss and heat production of the animal (Fig. 1a). We aimed to estimate the parameters G , T_R and H from the experimental observations. In the experiment, the controllable parameter was T_A and the observable parameters were T_B and VO_2 . Therefore, we first fitted the experimental results to linear models, equations (1, 2 and 5), and estimated a_1 , a_2 , b_1 , b_2 and G by MCMC sampling. For priors, a_1 , a_2 and G used log-normal distribution (natural logarithm of the variables were normally distributed by mean of 0 and standard deviation of 1) and the intercepts b_1 and b_2 used uniform distribution. Because T_R and H can be described as equation (7), they can also be described as equations (10) and (11). Introducing the posterior distribution of a_1 , a_2 , b_1 and b_2 , we estimated the posterior distribution of T_R and H . See Supplementary Source Code 2 for further information.

To compare the estimated parameters with past reports, we referenced the T_R and H of hibernators from three studies^{8,9,17}. We assumed 5.3 cal of energy is equivalent to consumption of 1 ml of oxygen and 1 cal = 4.184 J was applied for unit conversion.

Calculation of Q_{10} temperature coefficient of oxygen consumption rate. The Q_{10} temperature coefficient of oxygen consumption rate among normal and torpid condition was calculated in the following equation:

$$Q_{10} = \left(\frac{VO_{2,normal}}{VO_{2,torpor}} \right)^{10/(T_{B,normal} - T_{B,torpor})} \quad (21)$$

Because most biological reactions proceed with a Q_{10} of ~ 2 or 3^{39} , if the Q_{10} during torpor is larger than this, the decrease of oxygen consumption rate cannot be explained by simple temperature effect; rather, it can be assumed that the metabolism was suppressed actively.

References

- Geiser, F. Hibernation. *Curr. Biol.* **23**, R188–R193 (2013).
- Heldmaier, G., Ortmann, S. & Elvert, R. Natural hypometabolism during hibernation and daily torpor in mammals. *Respir. Physiol. Neurobiol.* **141**, 317–329 (2004).
- Andrews, M. T. Advances in molecular biology of hibernation in mammals. *Bioessays* **29**, 431–440 (2007).
- Carey, H. V., Andrews, M. T. & Martin, S. L. Mammalian hibernation: cellular and molecular responses to depressed metabolism and low temperature. *Physiol. Rev.* **83**, 1153–1181 (2003).
- Boutilier, R. G. Mechanisms of cell survival in hypoxia and hypothermia. *J. Exp. Biol.* **204**, 3171–3181 (2001).
- Neutelings, T., Lambert, C. A., Nusgens, B. V. & Colige, A. C. Effects of Mild Cold Shock (25°C) Followed by Warming Up at 37°C on the Cellular Stress Response. *PLoS One* **8**, e69687 (2013).
- Tamura, Y., Shintani, M., Nakamura, A., Monden, M. & Shiomi, H. Phase-specific central regulatory systems of hibernation in Syrian hamsters. *Brain Res.* **1045**, 88–96 (2005).
- Heller, H. C. & Colliver, G. W. CNS regulation of body temperature during hibernation. *Am. J. Physiol.* **227**, 583–589 (1974).
- Florant, G. L. & Heller, H. C. CNS regulation of body temperature in euthermic and hibernating marmots (*Marmota flaviventris*). *Am. J. Physiol.* **232**, R203–R208 (1977).
- Hudson, J. & Scott, I. Daily torpor in the laboratory mouse, *Mus musculus* var. albino. *Physiol. Zool.* **52**, 205–218 (1979).
- Willis, C. K. R. An energy-based body temperature threshold between torpor and normothermia for small mammals. *Physiol. Biochem. Zool.* **80**, 643–651 (2007).
- Snyder, G. K. & Nestler, J. R. Relationships between body temperature, thermal conductance, Q_{10} and energy metabolism during daily torpor and hibernation in rodents. *J. Comp. Physiol. B.* **159**, 667–675 (1990).
- Ortmann, S. & Heldmaier, G. Regulation of body temperature and energy requirements of hibernating alpine marmots (*Marmota marmota*). *Am. J. Physiol. Regul. Integr. Comp. Physiol.* **278**, R698–R704 (2000).
- Kanosue, K., Crawshaw, L. I., Nagashima, K. & Yoda, T. Concepts to utilize in describing thermoregulation and neurophysiological evidence for how the system works. *Eur. J. Appl. Physiol.* **109**, 5–11 (2010).
- Romanovsky, A. A. Thermoregulation: the roman concepts have changed. Functional architecture of the thermoregulatory system. *Am. J. Physiol. Regul. Integr. Comp. Physiol.* **292**, R37–R46 (2007).
- Hall, J. E. & Guyton, A. C. In *Guyton and Hall textbook of medical physiology*. at <http://www.us.elsevierhealth.com/guyton-and-hall-textbook-of-medical-physiology-9781455770052.html> (2015).
- Heller, H. C., Colliver, G. W. & Anand, P. CNS regulation of body temperature in euthermic hibernators. *Am. J. Physiol.* **227**, 576–582 (1974).
- Dikic, D., Heldmaier, G. & Meyer, C. W. Induced torpor in different strains of laboratory mice. *Hypometabolism in Animals* 223–229 (2008).
- Morton, S. R. Torpor and nest-sharing in free-living *Sminthopsis crassicaudata* (Marsupialia) and *Mus musculus* (Rodentia). *J. Mammal.* **59**, 569–575 (1978).
- Gavrilova, O. *et al.* Torpor in mice is induced by both leptin-dependent and -independent mechanisms. *Proc. Natl. Acad. Sci. USA* **96**, 14623–14628 (1999).
- Himms-Hagen, J. Food restriction increases torpor and improves brown adipose tissue thermogenesis in ob/ob mice. *Am. J. Physiol.* **248**, E531–E539 (1985).
- Iliff, B. W. & Swoap, S. J. Central adenosine receptor signaling is necessary for daily torpor in mice. *Am. J. Physiol. Regul. Integr. Comp. Physiol.* **303**, R477–R484 (2012).
- Bechtold, D. A. *et al.* A role for the melatonin-related receptor GPR50 in leptin signaling, adaptive thermogenesis, and torpor. *Curr. Biol.* **22**, 70–77 (2012).
- Gilbert, R. E. *et al.* SIRT1 activation ameliorates hyperglycaemia by inducing a torpor-like state in an obese mouse model of type 2 diabetes. *Diabetologia* **58**, 819–827 (2015).
- Swoap, S. J. The pharmacology and molecular mechanisms underlying temperature regulation and torpor. *Biochem. Pharmacol.* **76**, 817–824 (2008).
- Swoap, S. J. & Gutilla, M. J. Cardiovascular changes during daily torpor in the laboratory mouse. *Am. J. Physiol. Regul. Integr. Comp. Physiol.* **297**, R769–R774 (2009).
- Fang, J. & Fishbein, W. Sex differences in paradoxical sleep: influences of estrus cycle and ovariectomy. *Brain Res.* **734**, 275–285 (1996).
- Branchey, M., Branchey, L. & Nadler, R. D. Effects of estrogen and progesterone on sleep patterns of female rats. *Physiology & Behavior* **6** (1971).
- Nakamura, K. Central circuitries for body temperature regulation and fever. *AJP: Regulatory, Integrative and Comparative Physiology* **301**, R1207–R1228 (2011).
- Hamel, E. J. O., Grewe, B. F., Parker, J. G. & Schnitzer, M. J. Cellular Level Brain Imaging in Behaving Mammals: An Engineering Approach. *Neuron* **86**, 140–159 (2015).
- Susaki, E. A. *et al.* Whole-brain imaging with single-cell resolution using chemical cocktails and computational analysis. *Cell* **157**, 726–739 (2014).
- Fassbender, K. *et al.* Streamlining of prehospital stroke management: The golden hour. *Lancet Neurol.* **12**, 585–596 (2013).
- Dausmann, K. H., Glos, J., Ganzhorn, J. U. & Heldmaier, G. Physiology: Hibernation in a tropical primate - Even in the wound-down hibernating state, this lemur can warm up without waking up. *Nature* **429**, 825–826 (2004).
- Ruf, T., Streicher, U., Stalder, G. L., Nadler, T. & Walzer, C. Hibernation in the pygmy slow loris (*Nycticebus pygmaeus*): multiday torpor in primates is not restricted to Madagascar. *Sci. Rep.* **5**, 17392 (2015).
- Stan Development Team. Stan: A C++ Library for Probability and Sampling. at <http://mc-stan.org/> (2016).
- Stan Development Team. RStan: the R interface to Stan. at <http://mc-stan.org/> (2016).
- R Core Team. R: A language and environment for statistical computing. at <https://www.r-project.org/> (2016).
- McElreath, R. *Statistical Rethinking: A Bayesian Course with Examples in R and Stan.* (CRC Press, 2016).
- Reyes, B. A., Pendergast, J. S. & Yamazaki, S. Mammalian peripheral circadian oscillators are temperature compensated. *J. Biol. Rhythms* **23**, 95–98 (2008).

Acknowledgements

We thank the LARGE, RIKEN CDB for housing the mice. We also thank Takeshi Sakurai, Michiko Mandai and Take Matsuyama for insightful comments. This work was supported by a Grant-in-Aid for Young Scientists (B) (Grant No. 26870858, G.A.S.).

Author Contributions

G.A.S. designed the study and performed the experiments and analyses. G.A.S. and M.T. wrote the manuscript.

Additional Information

Supplementary information accompanies this paper at <http://www.nature.com/srep>

Competing financial interests: The authors declare no competing financial interests.

How to cite this article: Sunagawa, G. A. and Takahashi, M. Hypometabolism during Daily Torpor in Mice is Dominated by Reduction in the Sensitivity of the Thermoregulatory System. *Sci. Rep.* **6**, 37011; doi: 10.1038/srep37011 (2016).

Publisher's note: Springer Nature remains neutral with regard to jurisdictional claims in published maps and institutional affiliations.



This work is licensed under a Creative Commons Attribution 4.0 International License. The images or other third party material in this article are included in the article's Creative Commons license, unless indicated otherwise in the credit line; if the material is not included under the Creative Commons license, users will need to obtain permission from the license holder to reproduce the material. To view a copy of this license, visit <http://creativecommons.org/licenses/by/4.0/>

© The Author(s) 2016